19th Australasian Fluid Mechanics Conference
Melbourne, Australia
8-11 December 2014

Statistical Development of Wind Turbine Wakes for the Fully Developed Wind Turbine Array Boundary Layer Characterized via Wall-Normal-Spanwise Planes

N.M. Hamilton[1] and R.B. Cal[1]

[1]Department of Mechanical and Materials Engineering
Portland State University, Portland,Oregon, 97201, USA

Abstract

An experiment was conducted to investigate the development of a wind turbine wake in the fully developed turbine array. For a standard Cartesian wind turbine array, wake dynamics become independent of location in the wind farm after the fourth row, indicating a fully developed condition. Velocity fields oriented normal to the mean convective flow were measured using stereo particle image velocimetry in forward scatter. Measurements were made every half rotor-diameter (6cm) in the wake, $0.5 \leq x/D \leq 7.0$, to detail the dynamics in both the near and far wake regions. Measurements at each downstream location span a region larger than the swept area of the rotors. Statistics indicate that the mean flow is nearly axisymmetric in the near wake ($x/D \leq 3.0$), then show trends vertically upward, convected by the mean vertical velocity. The full Reynolds stress tensor is available through SPIV measurements and shows that very near to the turbine ($x/D \leq 1.0$), the presence of the mast and rotor blades have a large influence over the stress fields. The resupply of kinetic energy to the momentum deficit area of the wake is well characterized through the flux of kinetic energy. Velocity measurements are assessed in a cylindrical coordinate system with the central axis aligned with the hub of the wind turbine to observe the dependence on the passage of the rotor. In this frame of reference turbulence phenomena are assessed in a more natural sense as products of axial, radial, and azimuthal components of the flow.

Introduction

Wind turbine wakes for individual devices have been well characterized by previous research (e.g. [11, 13]). However, as wind energy becomes a more viable supplement to the overall energy production, wind turbines are being placed in larger and larger arrays. In such a case, the interaction between wakes becomes a topic of interest in order to ensure that global efficiency and productivity remain at acceptable levels. Complex flow generated by atmospheric forcing interacting with rotating blades is still the subject of interest in making wind energy more productive and efficient to help meet the increasing energy demands.

Large eddy simulations [2, 8, 9, 10, 12] have provided a platform for accessing full wakes and wake interaction in infinite wind turbine arrays. The idea of the 'infinite' array of wind turbines arises from periodicity of turbulence statistics in regularly arranged wind farms beyond the fourth row of devices [2, 3]. The periodicity in the streamwise spatial coordinate allows the convective and pressure gradient terms to be effectively omitted from the energy balance for wind turbine wakes.

The flux of kinetic energy, responsible for much of the resupply of high-momentum flow into the wake [1, 5, 4], is formulated with turbulent shear stresses combining radial and axial fluctuations of velocity. It is understood that the flux of kinetic energy is associated with large-scale turbulent structures in the wakes [6]. The production of turbulence is also important to the energy balance in the fully developed turbine array. Although short-lived in the wake, this quantity is often representative of energy made unavailable to successive turbines in the array.

In the current work measurements are made in a wind tunnel spanning the wake of a wind turbine model in a fully developed wind turbine canopy. Asymmetry is visible across wakes; statistics are reviewed in a polar-cylindrical coordinate system which may be more natural given the geometry of the turbines and flow. The flux of kinetic energy can then be viewed as inward or outward rather than vertical or lateral. The production of turbulence is formulated with gradients along the radial component, effectively including both the vertical and transverse contributions.

Theory

The mean kinetic energy equation in a wind turbine boundary layer can be described through a slightly modified set of turbulent boundary layer equations.

$$U_j \frac{\partial \frac{1}{2} U_i^2}{\partial x_j} = -\frac{U_i}{\rho} \frac{\partial P}{\partial x_i} + \overline{u_i u_j} \frac{\partial U_i}{\partial x_j} - \frac{\partial \overline{u_i u_j} U_i}{\partial x_j} - \mathcal{F}_{x_i} \qquad (1)$$

Above, the forcing term $\mathcal{F}_{x_i}$ represents the thrust force added to the flow as power is extracted by the wind turbine device. In many studies of wind turbine wakes [1, 5, 4, 7] the unsteady term is omitted from the mean kinetic energy budget through ensemble averaging of a large set of random samples in the period flow of wake. With the infinite array assumption equation (1) reduces to a balance between the flux of kinetic energy, the production of turbulence, and the thrust force from the wind turbine.

In the standard Cartesian formulation, the flux of kinetic energy and production terms from equation 1 require many components to describe motion into or out of the wake. For this reason, a polar-cylindrical coordinate system, with axis fixed at the hub of the rotor is a more natural choice as it enables analysis in a radial sense. Converting the stress tensor from the Cartesian to polar coordinate system can be achieved directly as,

$$R_{\text{polar}} = T R_{\text{cart}} T^{-1} \qquad (2)$$

where T is a transformation matrix,

$$T = \begin{bmatrix} cos\theta & sin\theta & 0 \\ -sin\theta & cos\theta & 0 \\ 0 & 0 & 1 \end{bmatrix} \qquad (3)$$

Analogous transformations can be applied to the flux of kinetic energy and production tensors yield the quantities of interest.

Experiment

Measurements of a wind turbine wake in the fully developed canopy layer were made in the wind tunnel furnished with a passive grid to introduce turbulence, removable vertical strakes shaped to precondition the boundary layer to in the wind tunnel to more closely match observed the atmospheric boundary

layer, and surface roughness via small-diameter chains. Characteristics of the inflow including mean velocity and turbulence intensity are shown in figure 1. In the rotor area of the approach, turbulence intensity in the streamwise direction is approximately 15% and is greater than those in spanwise or wall normal directions. The reader is referred to Hamilton, et al. [4] for a more complete description of the modeled approach flow.

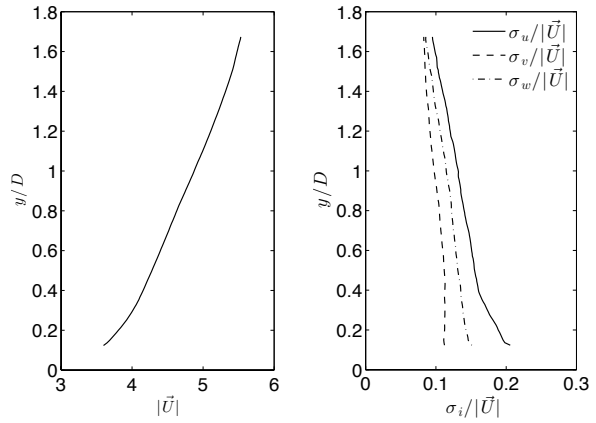

Figure 1: Profiles of mean velocity and turbulence intensity characterizing inflow to the model array.

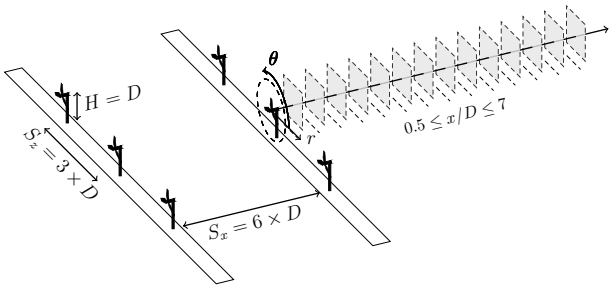

Figure 2: Schematic of a model wind turbine with and measurement planes across the wake. Flow is from left to right. Only the last two rows of wind turbines are shown in the schematic.

Figure 2 describes a turbine from the experiment. Measurement locations accessed through $2D-3C$ stereographic particle image velocimetry (SPIV) are shown as well as the polar-cylindrical coordinate system used in the following analysis. Measurements were made behind a wind turbine in the fully developed region, the fourth row for arrays arranged in a Cartesian grid. Rows of turbines were spaced six rotor diameters apart (72 cm) and columns separated by 3 rotor diameters (36 cm) hub-to-hub.

The wind turbine models consisted of a hollow steel mast and rotor blades cut from 0.0005 m sheet steel. The blades of the turbine were given pitch and twist via a press to ensure uniformity. Each blade was pitched $\gamma_{\text{root}} = 22^\circ$ out of the rotor plane at the root of the blade and had a 7° twist from root to tip, resulting in a pitch of $\gamma_{\text{tip}} 15^\circ$ at the tip of each blade. The nacelle of each turbine was a DC electric motor loaded with resistors to slow rotation of the blades, allowing each row of turbines to operate at its peak power coefficient. Figure 3 shows details of the model wind turbines.

Results

The mean axial velocity in the wake is shown in figure 5. Momentum deficit is evident throughout the wake. By $x/D = 5$, U_x increases monotonically in a wall-normal sense. Asymmetry expected in the wake of a rotating solid body is not seen in the axial velocity but is evident in the radial and tangential velocities (not shown here for brevity). In the far wake $x/D \geq 3.5$, gradients in the mean velocity soften and the stress fields become roughly axisymmetric. In the far wake of the wind turbine, the flow is well mixed and becomes more homogeneous, with vertical and spanwise velocities on the order of 5% of the hub height approach flow velocity.

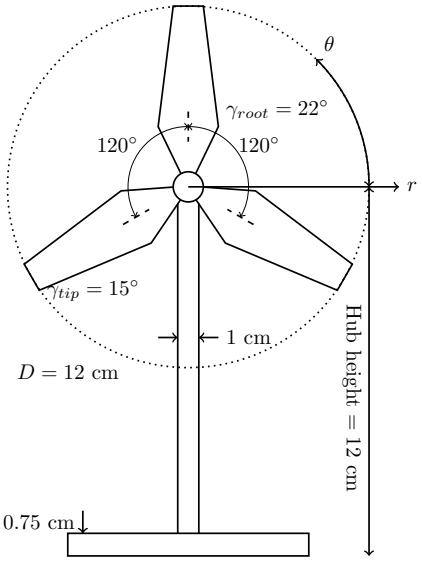

Figure 3: Schematic of a fully assembled wind turbine model including the mast and a section of the mounting plate. Polar-cylindrical coordinates r and θ are indicated for the radial and azimuthal components, respectfully. The axial component is aligned with the shaft of the turbine away from the reader.

Using SPIV yields simultaneous measurements of all three components of velocity and the full turbulent stress tensor. Past explorations of wind turbine wakes in similar arrays have focused on measurements in planes that are parallel to the mean flow, and miss many of the three-dimensional effects arising from the passage of the blades. Asymmetry in many of the stresses can be seen across the measurement planes throughout the near wake. Beyond $x/D \geq 4$ the wake begins to meander or shift away from the hub. Figure 4 shows two of the Reynolds shear stresses in the near wake an asymmetry arising from the passage of the rotor blades. Figures representing the flux and production effectively incorporate contributions from both Reynolds stresses shown.

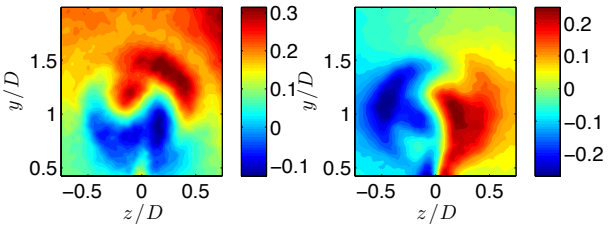

Figure 4: Reynolds shear stresses $-\overline{uv}$ (left) and $-\overline{uw}$ (right) at $x/D = 0.5$ show asymmetry that contributes to uneven flux of kinetic energy and production, $\overline{u_i u_j} U_i$ and $\overline{u_i u_j} \frac{\partial U_i}{\partial x_j}$, respectively.

Typically, the flux of kinetic energy is discussed as it pertains to the vertical entrainment of high-momentum flow from outside the wake [1, 5, 6]. The current measurements show that lateral transport from the sides of the wake is also significant.

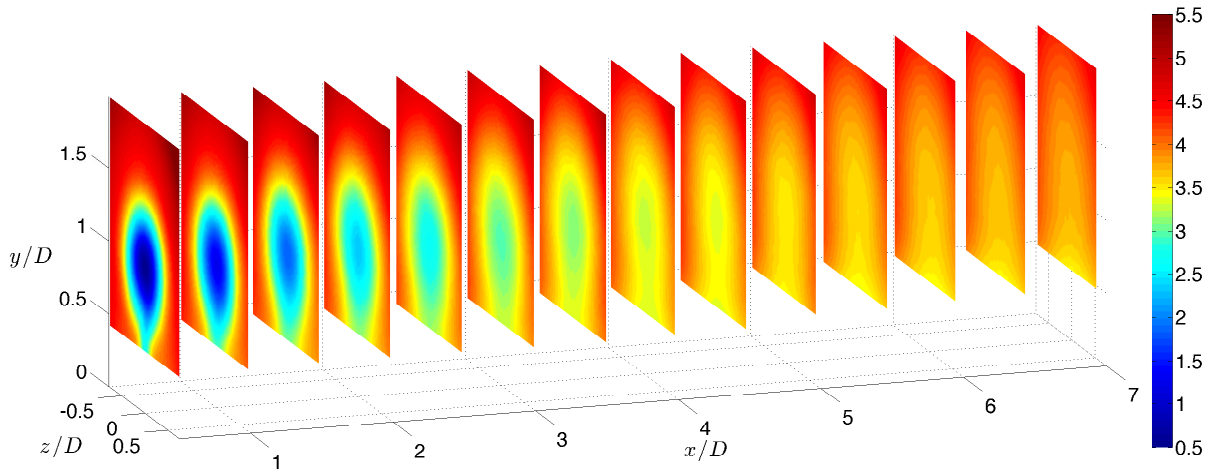

Figure 5: Mean axial (streamwise) velocity in the wake of a model wind tubine. Momentum deficit is seen in all measurement locations. U_x increases monotonically after $x_D = 5$.

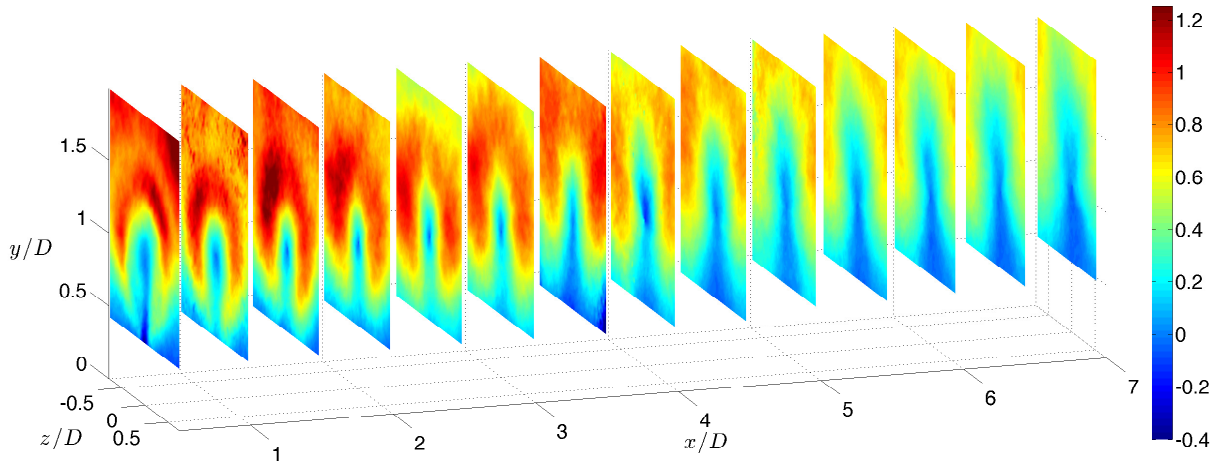

Figure 6: The flux of kinetic energy radially inward toward the center of the wake at $r = 0$. Positive values indicate inward entrainment of high-momentum flow. Formulation in cylindrical coordinates combines the vertical and lateral fluxes discussed in Cartesian coordinate systems.

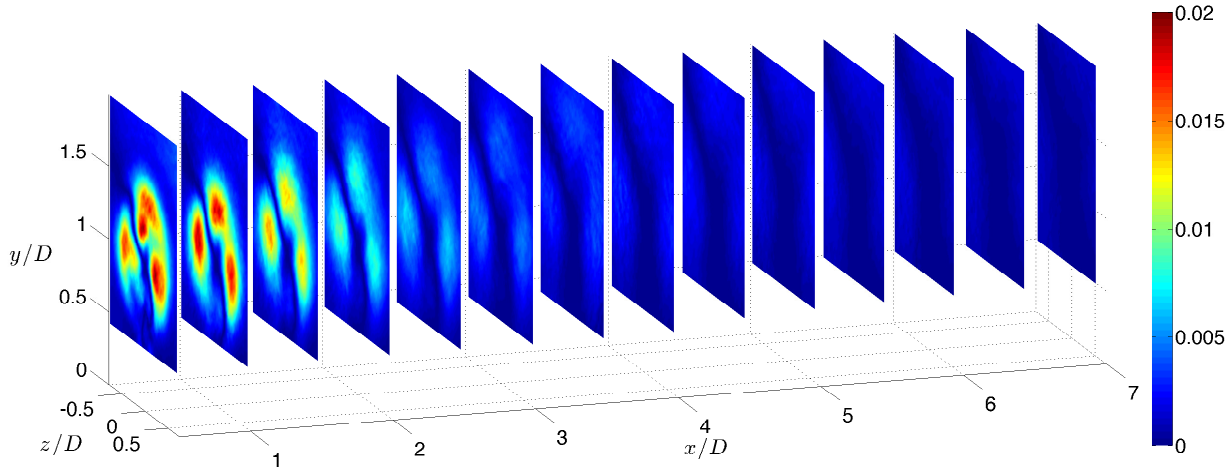

Figure 7: Production of turbulence $P_{xr} = \overline{u_x u_r} \frac{\partial U_x}{\partial r}$ combining the axial-radial Reynolds stress and gradients of the axial mean velocity with respect to the radial coordinate.

In experiments exploring the effects of streamwise and transverse spacing of wind turbines indicates that the lateral flux of kinetic energy is a function of spacing across the mean atmospheric flow. The flux of kinetic energy shown in figure 6 is the product of the mean axial velocity and the Reynolds shear stress combining fluctuations of velocity in the axial and radial directions. The formulation of F_{xr} includes effects from both the stresses shown in figure 4. Positive values of F_{xr} are seen in nearly all measurement locations, indicating that high-momentum flow is being entrained radially inward from nearly all directions. The exception to this trend is seen directly following the turbine mast at $x/D = 0.5$ and near the bottom of the fields.

Transforming the production tensor requires a bit more care to correctly manage the gradients in its composition. A review of the constituent components of the production tensor indicates that peak values occur at $x/D = 1$ for the axial-radial component P_{xr}, with values a full order of magnitude greater than the others. When viewed in the Cartesian coordinate system common to previous research, the only component considered is the in-plane contribution P_{xy}. However, due to spanwise gradients in the mean velocity, the out of plane component P_{xz} is also significant. When measurements are made parallel to the main flow, gradients in the transverse direction are out of reach and these components must be neglected. Contours of the production P_{xr} are shown in figure 7. The peak value of production $P_{xr} \approx 0.02$ m^{2}s^{-2} occur at $x/D = 1$ trailing the top-dead-center blade location, $\theta = 90^\circ$. As gradients in the axial mean velocity soften ($x/D = 3.5$) the production is quickly reduced to nearly null values. The clover pattern in the contour plots arises from the distribution and symmetry of stresses seen in the wake.

Conclusions

The measurements taken in the current work illuminate velocities and turbulent stresses across the wake of a wind turbine in a fully developed wind farm. Reynolds normal and shear stresses demonstrate asymmetry in the near wake but become more uniform after $x/D = 3.5$. The two shear stresses that contribute most significantly to the flux of kinetic energy and production are both well resolved with the current measurements.

Typically the discussion of the flux term is in terms of vertical entrainment of high-momentum flow from above the turbine canopy. The current results confirm findings of previous studies that indicate the lateral transport is also significant but its contribution depends on the spacing of devices in an array. Viewing the flux term in a polar-cylindrical coordinate system changes the discussion to entrainment inward toward along the radial coordinate from all directions. From this perspective a more complete view of the entrainment is attained.

Production of turbulence and the flux of kinetic energy balance the thrust force added to the flow in the infinite wind farm. In the adopted coordinate system the production shows activity across the wind turbine wake. This agrees with intuition as the shear stress $-\overline{uw}$ is on the same order as $-\overline{uv}$ and gradients of mean velocity horizontally across the wake are similar to those taken in the vertical direction.

Continued work with the current data will yield results pertaining to flux tubes according to the work undertaken by Meyers and Meneveau [10]. Identifying momentum flux pathways has implications in the design of future wind farms and simulation software to determine optimal placement of individual devices.

A parallel experiment investigating phase-dependent turbulence statistics is described for an identical experimental arrangement in *Characterization of turbulence and deterministic stresses through phase-dependent measurements in the near wake of a wind turbine in an infinite turbine array* by Hamilton and Cal, presented in the current conference.

References

[1] Cal, R. B., Lebrón, J., Castillo, L., Kang, H. S. and Meneveau, C., Experimental study of the horizontally averaged flow structure in a model wind-turbine array boundary layer, *Journal of Renewable and Sustainable Energy*, **2**, 2010, 013106.

[2] Calaf, M., Meneveau, C. and Meyers, J., Large eddy simulation study of fully developed wind-turbine array boundary layers, *Physics of Fluids*, **22**, 2010, 015110.

[3] Chamorro, L. P., Arndt, R. and Sotiropoulos, F., Reynolds number dependence of turbulence statistics in the wake of wind turbines, *Wind Energy*, **15**, 2012, 733–742.

[4] Hamilton, N., Cal, R. B. and Melius, M., Wind turbine boundary layer arrays for cartesian and staggered configurations: *Part I*, flow field and power measurements, *Wind Energy*, 2014, DOI:http://dx.doi.org/10.1002/we.1697.

[5] Hamilton, N., Kang, H. S., Meneveau, C. and Cal, R. B., Statistical analysis of kinetic energy entrainment in a model wind turbine array boundary layer, *Journal of Renewable and Sustainable Energy*, **4**, 2012, 063105.

[6] Hamilton, N., Tutkun, M. and Cal, R. B., Wind turbine boundary layer arrays for cartesian and staggered configurations: Part ii, low-dimensional representations via the proper orthogonal decomposition, *Wind Energy*, 2014, DOI:http://dx.doi.org/10.1002/we.1719..

[7] Lebrón, J., Castillo, L. and Meneveau, C., Experimental study of the kinetic energy budget in a wind turbine streamtube, *Journal of Turbulence*, **13**.

[8] McBean, G. and Elliott, J., The vertical transports of kinetic energy by turbulence and pressure in the boundary layer, *Journal of the Atmospheric Sciences*, **32**, 1975, 753–766.

[9] Meyers, J. and Meneveau, C., Optimal turbine spacing in fully developed wind farm boundary layers, *Wind Energy*, **15**, 2012, 305–317.

[10] Meyers, J. and Meneveau, C., Flow visualization using momentum and energy transport tubes and applications to turbulent flow in wind farms, *Journal of Fluid Mechanics*, **715**, 2013, 335–358.

[11] Snel, H., Review of aerodynamics for wind turbines, *Wind Energy*, **6**, 2003, 203–211.

[12] Troldborg, N., Larsen, G. C., Madsen, H. A., Hansen, K. S., Sørensen, J. N. and Mikkelsen, R., Numerical simulations of wake interaction between two wind turbines at various inflow conditions, *Wind Energy*, **14**, 2011, 859–876.

[13] Vermeer, L. J., Sørensen, J. N. and Crespo, A., Wind turbine wake aerodynamics, *Progress in aerospace sciences*, **39**, 2003, 467–510.